

Liquid Interfaces Probed by Second-Harmonic and Sum-Frequency Spectroscopy

K. B. Eisenthal

Department of Chemistry, Columbia University, New York, New York 10027

Received September 6, 1995 (Revised Manuscript Received March 13, 1996)

Contents

I. Introduction	1343
II. Equilibrium Properties at Liquid Interfaces	1344
A. Molecular Orientational Structure Using SHG	1344
B. Absolute Orientation of Molecules—Polar Alignment	1346
C. Sum Frequency Generation—An Interface Vibrational Spectroscopy	1347
D. Chemical Reactions at Interfaces	1348
E. Electrochemistry	1350
F. Some Environmentally Interesting SH Studies	1351
G. Structural Phase Transitions	1351
H. Chiral Interfaces	1353
III. Dynamics at Liquid Interfaces	1354
A. Adsorption Kinetics to Air/Water Interfaces	1354
B. Electron Transfer at a Liquid/Liquid Interface	1355
C. Photoisomerization at Aqueous Interfaces	1355
D. Orientational Relaxation at the Air/Water Interface	1357
E. Photogeneration of Charges at a Semiconductor/Water Electrochemical Interface	1358
F. Dynamics of Intermolecular Energy Transfer	1358
IV. Summary	1359
V. Acknowledgments	1359
VI. References	1359



Kenneth B. Eisenthal received a B.S. in chemistry from Brooklyn College and an M.A. in physics and Ph.D. in chemical physics from Harvard University. He did postdoctoral research at UCLA and was at IBM Almaden before coming to Columbia University in 1975.

dimension, is the underlying factor that determines the chemical composition, structure, dielectric, and transport properties of an interface, all of which differ markedly from either of the bulk media that bound it. Because of the unique chemical, physical, and biological properties of interfaces there is enormous interest in them in both the basic sciences and in medicine (membrane binding and transport), engineering (etching of computer chips, lubrication), and increasingly the environmental sciences (air/water, soil/water, and air/stratospheric ice interfaces).⁹ Despite the recognized importance of interfaces it had been extremely difficult to bring the powerful methods of spectroscopy to bear on interfacial problems. The problem was that traditional spectroscopic methods, such as absorption, emission, and Raman scattering, are generally not able to differentiate optical signals originating from surface versus bulk species. If the species of interest is present in the bulk as well as the interface then the optical signals due to absorption, fluorescence, and Raman scattering will almost always be dominated by the overwhelmingly larger number of bulk molecules.

The reason that second-harmonic and sum-frequency generation can selectively probe interfaces, without being overwhelmed by bulk species, is that these second-order processes are electric dipole forbidden in centrosymmetric media.^{1–7} Therefore, in this approximation, bulk liquids, gases, and amorphous and centrosymmetric crystalline solids do not generate second-harmonic and sum-frequency signals. At the interface, on the other hand, the molecular and atomic species experience different interactions in the up vs the down directions. Thus

I. Introduction

A powerful approach to the study of interfaces has been developing rapidly in the past decade. It is based on the spectroscopic methods of second-harmonic (SHG) and sum-frequency generation (SFG).^{1,2} These nonlinear optical techniques, being spectroscopic, provide information at the most fundamental level.^{1–8} A microscopic description of equilibrium and dynamic interface processes requires knowledge of the molecules at the interface, their orientational structure, the energetics that drive chemical and physical processes, and the time scale of molecular motions and relaxation processes. The techniques of second-harmonic and sum-frequency generation have made it possible to selectively probe the chemistry, physics, and biology of gas/liquid, liquid/liquid, liquid/solid, gas/solid, and solid/solid interfaces at the molecular level.

The special properties of interfaces responsible for their importance and widespread interest, arise from the asymmetry in forces that molecular and atomic species experience there. The asymmetry inherent to an interface, together with its molecularly thin

inversion symmetry, which is present in the bulk, is broken at the interface. There are some physical situations where higher order terms such as electric quadrupole interfacial and bulk contributions must be considered. When these cases arise we will take note of them.

The generation of the second-harmonic and sum-frequency light, which makes it possible to selectively probe the interface, can be described in terms of the polarization induced in the interface by the incoming light. The induced polarization that leads to second harmonic and sum frequency generation is the second-order polarization $P^{(2)}$.^{1,2} It is proportional to the product of the incident light fields and thus oscillates at their sum and difference frequencies. In this discussion we will consider only sum-frequency generation, for which there are two incident light fields at the interface, one centered at ω_1 and the other at ω_2 , and second-harmonic generation, which is the degenerate sum frequency case, when there is only one incident light field, $\omega_1 = \omega_2$. The sum-frequency light field generated at $\omega_1 + \omega_2$ can be thought of as arising from the oscillating polarization $P^{(2)}_{\omega_1+\omega_2}$

$$P^{(2)}_{\omega_1+\omega_2} = \chi^{(2)}_{\omega_1+\omega_2} E_{\omega_1} E_{\omega_2} \quad (1)$$

where E_{ω_1} and E_{ω_2} are the incident light fields and $\chi^{(2)}_{\omega_1+\omega_2}$ is the second-order nonlinear susceptibility, which contains all of the information on the chemical species comprising the interface. In order to analyze the second-harmonic and sum-frequency signals, the contributions of the various interfacial species to the nonlinear susceptibility $\chi^{(2)}$ must be established. In a general way $\chi^{(2)}$ can be expressed as the sum over the nonlinear susceptibility $\chi_i^{(2)}$ for each of the species i at the interface. In many cases the molecules of interest, often called the adsorbates, make the dominant contribution to $\chi^{(2)}$ because of their larger intrinsic nonlinearity at the fundamental and harmonic light frequencies selected for the experiments. In the case of metals, the metal surface often has a larger nonlinearity than that of the adsorbates. The adsorbate population and interactions with the metal surface are then monitored by the change in the second-harmonic signal induced by the adsorbates.

In order to relate the macroscopic quantity $\chi^{(2)}$ to the molecules that make up the interface, an approximation of weak interactions between the adsorbates is often made

$$\chi^{(2)} = N_s \langle \alpha^{(2)} \rangle_{\text{OR}} \quad (2)$$

where N_s is the number of adsorbates per centimeter squared, and $\alpha^{(2)}$ is the molecular second-order polarizability, sometimes referred to as the hyperpolarizability. The brackets $\langle \rangle_{\text{OR}}$ indicates an orientational average over the interface molecules. In those cases where more than one molecular species is contributing to the second-harmonic or sum-frequency susceptibility $\chi^{(2)}$, then the sum over the number density N_{s_i} and $\alpha_i^{(2)}$ for each of the species i is required. The quantity $\alpha^{(2)}$ is a sum over a product of transition matrix elements between the electronic, vibrational states of the molecule. It also contains frequency-dependent denominators, which can go

into resonance and greatly enhance the SH and SF signals, when electronic and or vibrational transition frequencies become equal to the frequencies of the fundamental, second-harmonic, or sum-frequency light fields.^{9a}

The intensity of the sum-frequency signal $I(\omega_1 + \omega_2)$ can be written as

$$I(\omega_1 + \omega_2) \propto |\hat{e}(\omega_1 + \omega_2) \cdot \chi^{(2)} : \hat{e}(\omega_1) \hat{e}(\omega_2)|^2 I(\omega_1) I(\omega_2) \quad (3)$$

where $\hat{e}(\omega_1 + \omega_2)$ is the unit vector for the polarization of the light field at $\omega_1 + \omega_2$, and $I(\omega_1)$, $I(\omega_2)$ are the intensities of the incident light fields. Because $\chi^{(2)}$ is proportional to the number density N_s , the generated sum-frequency and second-harmonic signals, which are proportional to $|\chi^{(2)}|^2$, scale with the square of the density. This N_s^2 dependence is obtained when only one interface species dominates the generated optical signals; otherwise, a different dependence is found. The second-harmonic and sum-frequency radiation are analyzed in terms of the strength of their signals, which gives interface population information, the frequency dependence of optical signals, which yields information on the molecule's electronic and vibrational energy levels at the interface, the polarization direction of the generated light field, which yields information on interfacial molecular orientation, the phase of the generated light field, which provides information on the absolute orientation of the molecule (polar alignment), and the change in all of these measured quantities with time, which yields information on intra and intermolecular dynamic processes.

In this abbreviated article only liquid interfaces will be considered; gas/solid and solid/solid interfaces are not included. This restriction is necessary because of the enormous increase in SH and SF studies in recent years, which makes it extremely difficult to properly discuss the range of work being carried out around the world. Unfortunately not all of the fine work even in the area of liquid interfaces has been included because of both space and time limitations. A number of review articles are referred to which cover some of the research material not covered in this article.³⁻⁸

II. Equilibrium Properties at Liquid Interfaces

A. Molecular Orientational Structure Using SHG

The geometrical arrangement of molecules at an interface, which we refer to as orientational structure, is of key importance to any microscopic description of the chemical, physical, and biological properties of interfaces. The interface structure is determined by the intermolecular forces among the adsorbates and the molecules in the adjacent phases. The orientation-determining forces range from electrostatic and hydrogen-bonding forces, to hydrophilic solvation and hydrophobic repulsions. The interface orientational information is contained in the relation between the elements of $\chi^{(2)}$, which are measured in the SH experiments, and the molecular hyperpolarizability $\alpha^{(2)}$. As a simple example assume a single element $\alpha^{(2)}_{zzz}$, where z is a molecular axis, dominates

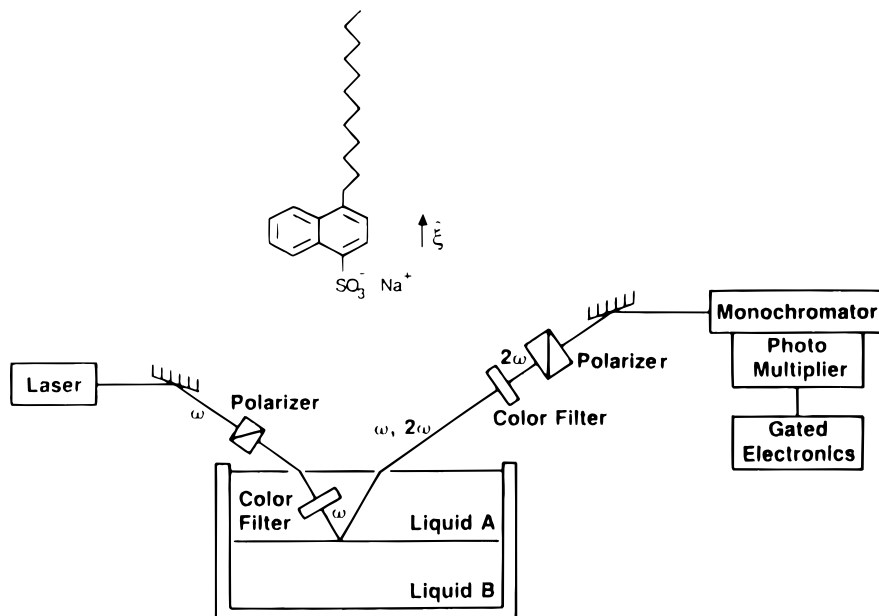


Figure 1. Schematic of apparatus to observe monolayers at a liquid/liquid interfaces using second-harmonic generation. The structure of sodium 1-dodecyl naphthalene-4-sulfonate is shown. (Reprinted from ref 34. Copyright 1988 American Chemical Society.)

the SH signal. Two of the three allowed $\chi^{(2)}$ elements at an interface bounded by centrosymmetric bulk media are

$$\chi_{ZZZ}^{(2)} = N_s \alpha_{zzz}^{(2)} \langle \cos^3 \theta \rangle_{OR}$$

$$\chi_{XZX}^{(2)} = \frac{1}{2} N_s \alpha_{zzz}^{(2)} \langle \cos \theta \sin^2 \theta \rangle_{OR} \quad (4)$$

where θ is the angle between the molecular z axis and the interface normal axis Z . We thus see that measurements of these elements or some ratio of all of the allowed $\chi^{(2)}$ elements, e.g. by measuring the polarization of the SH light, yields an expression in terms of the orientational angle θ .

1. Experiment and Theory of Small Molecule Orientation

The pioneering second-harmonic experiments on molecular orientation were carried out on *p*-nitrobenzoic acid ($\text{NO}_2\text{-C}_6\text{H}_4\text{-COOH}$) molecules adsorbed to the air/silica and ethanol/silica interfaces.¹⁰ Assuming a narrow distribution of orientations it was found that the orientation of the long axis with respect to the surface normal was about 70° at the air/silica interface. However at a liquid(ethanol)/solid(silica) interface the molecule becomes more upright, going to an angle of 40° , which demonstrates the strong effects of solvation on orientation. The first SHG studies of the population, adsorption isotherm, and orientation of solute molecules adsorbed from a bulk solution to an air/solution interface were carried out on phenol ($\text{C}_6\text{H}_5\text{OH}$) molecules at the air/aqueous solution interface.¹¹ It was found that the phenol molecules have their long axes tilted by 50° to the surface normal and, interestingly, that the molecular orientation did not change as the phenol interface density increased up to a full monolayer coverage. It appears that the orientation is controlled chiefly by the interaction of the hydroxy group of phenol with the water subphase and not with the laterally positioned molecules of the interface.

The interplay between theory and experiment is crucial to the rapid and full development of a research field. It is good to see that various powerful calculation methods are increasingly being brought to bear on interface problems.^{12-32a,b} A molecular dynamics simulation of phenol at the vapor/water interface²⁶ predicts a fairly broad orientational distribution centered about 45° , which is in good agreement with the experimental SHG result of 50° . In these studies a single element of $\alpha^{(2)}$ was assumed to be of dominant importance. However more than one element of $\alpha^{(2)}$ can contribute and should be included in the analysis of orientational data. An example where this has been done is *p*-nitrophenol, $p\text{-NO}_2\text{-C}_6\text{H}_4\text{OH}$, at air/water^{33,33a} and heptane/water^{33a} interfaces. These studies suggest that the *p*-nitrophenol has a broad distribution centered at about 40° for both of these interfaces.

2. Molecules at Liquid/Liquid Interfaces

An important interface in environmental chemistry, membrane chemistry, and purification methodologies is the liquid/liquid interface. Second-harmonic generation has proven to be a powerful way to study these buried interfaces following the early work on the orientation of the naphthalene chromophore in the long-chain surfactant sodium 1-dodecyl naphthalene-4-sulfonate at the decane/water and water/carbon tetrachloride interfaces,³⁴ where it was shown that the adsorbate orientation strongly depends on the makeup of the interface (Figure 1). For the decane/water interface the angle between the short axis of the naphthalene chromophore and the interface normal was 21° , whereas for the water/ CCl_4 interface the angle shifted to 38° . Recent advances have used SHG to probe surfactants containing an aromatic head group at the water/dichloroethane interface in an electrochemical cell.³⁵ By varying the potential across the cell the population of the charged form of the surfactant at the interface could be

varied. Measurement of the magnitude of the SH signal showed that the interface population did vary with potential, whereas measurement of the polarization of the SH light showed that the surfactant orientation did not change with the applied potential.

3. Molecular Ordering at Liquid/Solid and Liquid/Liquid Interfaces

In general the SH signal contains both dipolar contributions and higher order contributions, in particular quadrupolar contributions. If the molecules at an interface are orientationally well ordered then the dipole part often dominates. However if there is considerable disorder, then the dipole contribution is reduced because of cancellation among the interfacial molecules. In this case electric quadrupole contributions become relatively more important. These qualitative ideas on the relative contributions of dipolar and quadrupolar contributions to the SH signal have been supported by studies at air/solid, liquid/solid, air/liquid, and liquid/liquid interfaces.^{36,36a} These qualitative ideas have now been taken a step further. It has been argued that deviations from Kleinman symmetry approximation, which relates the amplitude of the $\chi^{(2)}_{YZY}$ and $\chi^{(2)}_{ZYY}$ elements, can be used as a measure of interfacial ordering.³⁷ By using these arguments it has been suggested that the observed change in the ratio of the $\chi^{(2)}_{YZY}$ and $\chi^{(2)}_{ZYY}$ elements from a value close to 1.0 for the even number alkane (octane and decane)/water interfaces to a value of 1.3 to 1.5 for the odd number alkane (heptane and nonane)/water interfaces indicates less orientational order at the odd alkane interfaces. These inferences are most interesting and the possibility of the different alkanes controlling the interfacial ordering, as well as the use of the Kleinman approximation in molecular ordering, warrants further experimental and theoretical investigation.

4. Polymers at the Air/Water Interface

Polymers spread at interfaces have features that make them more attractive in some applications than a monolayer of small molecules. The increased chemical and physical stability, including the prevention of interface aggregation, has made these materials ones of increased interest. A SH study of a polymer monolayer and a monolayer of its monomeric precursor found that at the same surface pressure there was greater polar alignment and packing density for the polymer monolayer.^{37a} In a different polymer monolayer, poly(acrylonitrile-*co*-4-vinyl pyridine), at the air/water interface, phase measurements were used to gain information on the orientation of the pyridine chromophore and the coiling of the polymer chain.³⁸ Unlike the aforementioned polymers, where it was found that the orientation of the monomer units comprising the polymer chain changed as the density of the polymer increased, work on a polybutyl alcohol polymer^{38a} showed that the monomeric orientations did not change from a dilute to a high concentration regime. This constancy in the monomeric orientation indicates that the monomeric structure remains the same as the polymer concentration increased. Because of the con-

stancy of structure a scaling law for two dimensions can be applied. In so doing it was found for this polymer that a two-dimensional scaling law was obeyed, which is the first such demonstration for a polymer at a liquid interface. Why a scaling law is applicable to the polybutyl alcohol polymer and not the perfluoroalkyl or polyacrylonitrile polymers remains unknown at this time. Turning now to a SH study, which has implications in biological systems, we report on an interesting exchange behavior between a biopolymer (protein) and surfactants at the air/water interface.³⁹ The protein lipase was found to drive adsorbed surfactants into the water phase when the surfactant concentration was low, but at higher surfactant concentrations a double layer with the surfactant on top of the protein was observed.

B. Absolute Orientation of Molecules—Polar Alignment

Although measurement of the polarization of the SH or SF light provides information about the tilt angle of a molecule with respect to the interface normal, it cannot give the absolute orientation of the molecule, i.e. it does not reveal whether the molecule is pointing up vs down. In other words it does not give the molecular polar alignment. The determination of the absolute orientation by SHG was accomplished when it was recognized that the sign, more generally the phase, of the nonlinear susceptibility $\chi^{(2)}$ is dependent on the polar alignment of the interfacial molecules.⁴⁰ This is readily seen if we consider $\chi^{(2)}_{XZX}$ in eq 4. The sign of $\chi^{(2)}_{XZX}$ is determined by the product of the sign of $\alpha^{(2)}_{zzz}$ and that of $\langle \cos \theta \sin^2 \theta \rangle$. Thus if the sign of $\alpha^{(2)}_{zzz}$ is obtained from experiment or theory, and the sign of $\chi^{(2)}_{XZX}$ is obtained from the SH phase measurement, then the sign of $\langle \cos \theta \sin^2 \theta \rangle$ is determined. For example if $\alpha^{(2)}_{zzz}$ is negative and the measured value of $\chi^{(2)}_{XZX}$ is positive then $\langle \cos \theta \sin^2 \theta \rangle$ must be negative. This means that θ must be greater than $\pi/2$ and the molecular z axis is therefore directed downward with respect to the surface normal Z . Note that the polarization of the SH light is the same whether the molecular angle is θ or $\pi - \theta$, which is the reason why polarization only gives the tilt of the molecular axis and not its direction.

1. Phenols at the Air/Water Interface

The phase of $\chi^{(2)}_{XZX}$ was measured by an interference method and first applied to phenol (C_6H_5OH) at the air/water interface as a test case.⁴⁰ Phenol was selected because chemical insight strongly suggests that the OH group of phenol will point toward the water phase in order to be hydrogen bonded with the water molecules. The SH phase measurements indicated that the OH group points toward the bulk water phase, in agreement with chemical expectation, and thereby supports the validity of the method for absolute orientation determinations. The method was subsequently applied at air/water interfaces that contained *p*-nitrophenol and *p*-bromophenol, both of which have permanent molecular dipole moments directed in the opposite sense to phenol.⁴¹ The absolute phase measurements revealed that all of these phenols have their hydroxy group pointing

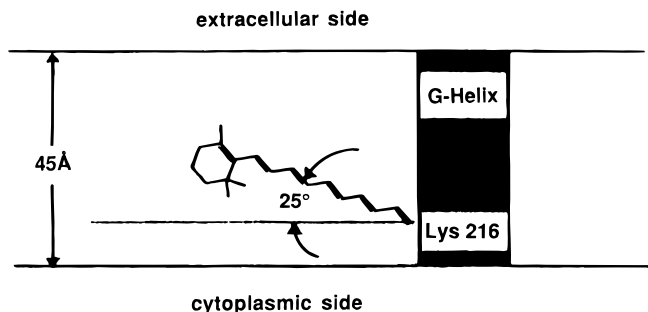
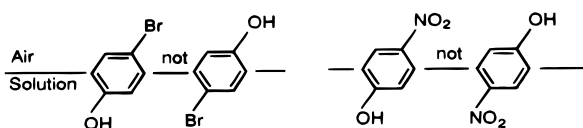


Figure 2. Absolute orientation of the retinal chromophore of bacteriorhodopsin in purple membrane obtained from second-harmonic phase measurement. (Reprinted from ref 42. Copyright 1989 American Institute of Physics.)

toward the bulk water, which establishes that it is the hydroxy group that controls the polar alignment, not the molecular dipole moment.



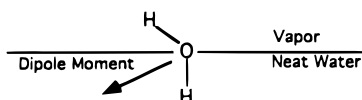
If instead of measuring the phase at a given frequency one measures the phase at many different frequencies, then the real and imaginary parts of $\chi^{(2)}$ as well as the phase of $\chi^{(2)}$ can be obtained.³³ The results of this frequency study are in accord with the aforementioned model of the polar alignment of *p*-nitrophenol having the OH projecting into the water.

2. Absolute Orientation of the Retinal Chromophore in a Biological Membrane

Light plays a crucial role in the physiology of halobacteria. Photoexcitation of the retinal chromophore in bacteriorhodopsin, which is contained in the purple membrane of the bacteria, causes a change in the charge distribution of the chromophore. The charge redistribution in turn leads to changes in the opsin protein conformation and finally the pumping of protons across the cell membrane. The absolute orientation of the retinal chromophore in the purple membrane is therefore important in effecting a change in the electrostatic potential across the membrane and generating a directional proton gradient. By using the SH interference method it was established that the ring part of the retinal chromophore pointed toward the extracellular side of the membrane⁴² (Figure 2).

3. Orientation of Water at the Air/Neat Water Interface

An interface of universal interest is the vapor/neat water interface. A key structural issue is the absolute orientation of the water molecules. On the average is the water dipole moment directed toward the bulk water phase, which would mean that the oxygen is pointing towards the vapor, or is it the opposite way?



The results obtained from various measurements of the interface electrostatic potential, which would give the absolute orientation of water, are not in agreement.^{43–48} On the theoretical side most calculations indicate that the oxygen is up, i.e. the dipole moment is down.^{13–17,20} From the SH phase measurements the preferred orientation of the water molecule was inferred to be the one where the dipole moment is down, in agreement with most calculations.⁴⁹ The relatively small SH signal for the vapor/neat water interface indicates a small value for $\chi^{(2)}$, which suggests that the dipole axes of the water molecules form a shallow angle with the surface horizontal, as schematically shown.

C. Sum Frequency Generation—An Interface Vibrational Spectroscopy

In a sum frequency experiment two beams of light, one at ω_1 and the other at ω_2 , overlap in space and time at an interface and generate radiation at the sum frequency, $\omega_1 + \omega_2$. If one of the beams is an infrared beam at a frequency ω_{IR} that matches the frequency of a molecular vibration, then a very large resonance enhancement of the SF signal is obtained.^{50,51} To be sum frequency active the vibrational mode must be one that is both IR and Raman active. By scanning the infrared frequency, keeping the frequency of the other beam constant, usually a visible beam, one obtains a vibrational spectrum of the molecules at the interface. The SF spectrum, which is a plot of SF intensity vs ω_{IR} , consists of a nonresonant background signal due to the electronic and the vibrational transitions that are not at the frequencies of the incoming visible and IR beams, and a number of peaks that are due to resonances at the vibrational frequencies of the interfacial molecules. Because SFG is a vibrational spectroscopy, unlike SHG which is an electronic spectroscopy, it has the fingerprint sensitivity to identify specific chromophores and thus can be more readily used to analyze the molecular composition of an interface. It is of particular value for liquid interfaces because electronic transitions at interfaces, as in bulk liquids, are generally broad and structureless, unlike the much narrower vibrational transitions. In addition to interfacial population information, SFG provides information on the orientation of the various vibrationally active chromophores and spectral information on their intermolecular interactions, such as hydrogen bonding.

1. Molecular Orientation and Spectra at Air/Neat Liquid Interfaces

SFG studies of a series of vapor/neat linear alcohol interfaces, from methanol (CH_3OH) through octanol [$\text{CH}_3-(\text{CH}_2)_7\text{OH}$] found for all of the alcohols that there was a broad distribution of orientations for the terminal methyl group, peaked about an angle less than 40° with respect to the surface normal.⁵² The absence of any orientational variation with the even vs odd number of carbons indicates that the chain axes have an orientational distribution centered about the interface normal. Measurements of the relative strengths of the methylene, CH_2 , and methyl, CH_3 , SFG signals demonstrated that unlike the

shorter chain alcohols, the longer alcohols, hexanol, heptanol, and octanol, have gauche as well as trans CH_2 conformations. This inference is based on the methylene signals being very weak when the alkyl chain is in an all-trans conformation, which however becomes strong for a gauche conformation. The SF spectra of the OH group suggests that the interface alcohol molecules form a more highly structured hydrogen-bonding network than is present in the bulk alcohol. A further interesting result was found on diluting methanol with water, where it was found that the methanol shifted to an orientation closer to the interface normal and extended over a significantly narrower distribution.⁵³ Apparently when methanol is surrounded by water molecules its hydrophobic methyl group minimizes water interactions by pointing closer to the normal to the interface.

2. Vapor/Neat Water Interface—Hydrogen Bonding of Water

The SFG spectrum of water at the air/neat water interface shows the presence of two types of OH groups.⁵⁴ One is not hydrogen bonded, which suggests that it is projecting into the air and comprises 20% of a full water monolayer. The remaining OH groups are hydrogen bonded and pointed into the bulk water. These results are consistent with the SH phase measurements⁴⁹ and the inferences from the SF and SH studies that the "average" orientation of water molecules, i.e. the orientation of the symmetry axis of water, which is the dipole moment axis of a water molecule, forms a small angle with the interface horizontal direction. See the sketch of the water orientation in Section I.B.3.

3. Interactions of Liquids with Hydrophobic/Hydrophilic Surfaces

In a series of SF experiments the detailed interactions between a monolayer of long-chain molecules with a number of liquids were investigated. The vibrational spectra in the range of C–H stretches were obtained for alkoxy terminated hexadecanethiols of varying length⁵⁵ $\text{CH}_3(\text{CH}_2)_n\text{O}(\text{CH}_2)_{16}\text{SH}$ ($n = 0-3$). The monolayers were bonded by the thiol group to silver and gold substrates and exposed to air, hexane, acetonitriles and water. A polar liquid such as acetonitrile was found to cause shifts in the SF peaks, especially in the $n = 0$ monolayer, but did not cause major changes in the orientational structure. With water, on the other hand, shifts and broadening were observed and attributed to the effects of hydrogen bonding of the ether oxygen with water (Figure 3). The decrease in SF intensity for the water interface provided evidence that there was significant structural perturbations of the monolayer, possibly due to an increased disorder near the top of the monolayer arising from hydrogen bonding of water that had penetrated to the partially buried oxygen of ether. A clear depth effect was observed in that the perturbations to the SF spectra decreased as the position of the ether chromophore moved further away from the liquid/monolayer interface. These SF experiments are of particular relevance to the phenomenon of wetting. By varying the position of the ether oxygen, with respect to the surface that

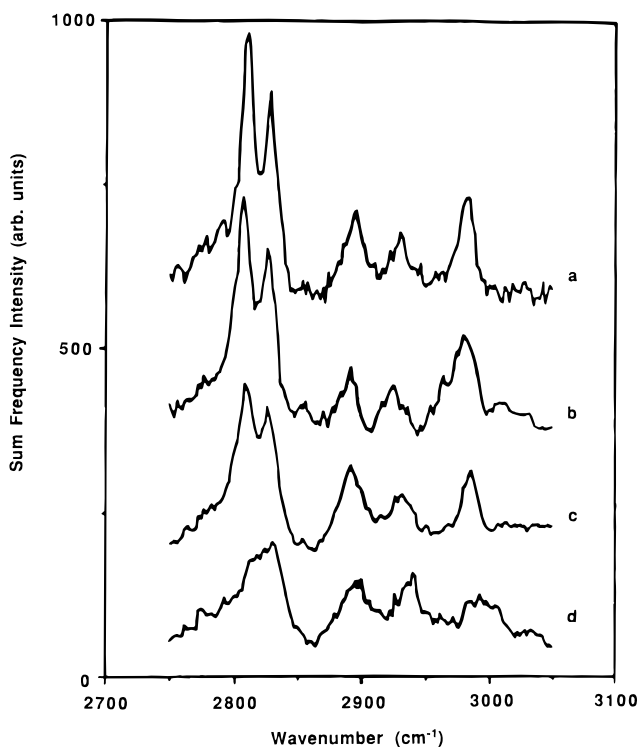


Figure 3. Vibrational spectra of 16-methoxyhexadecanethiol, $\text{CH}_3\text{O}(\text{CH}_2)_{16}\text{SH}$, on gold in contact with (a) air, (b) hexanol- d_{14} , (c) acetonitrile- d_3 , and (d) water, obtained from sum-frequency measurements. (Reprinted from ref 55. Copyright 1993 American Chemical Society.)

makes contact with the liquid, the hydrophilic/hydrophobic character of the surface is changed. In this and other studies of surfactants at hydrophobic surfaces the molecular interactions that underlie the phenomenon of wetting can be directly probed.^{56-58,58a}

4. Absolute Orientation from SFG Phase Measurements

Just as the phase of $\chi^{(2)}$ for second-harmonic generation can be used to obtain absolute molecular orientation, the phase of $\chi^{(2)}$ for sum-frequency generation can be used to obtain the absolute orientation of a given chromophore in a molecule. An appealing characteristic of the SF measurement is that the phase measurement yields the absolute orientation of each of the SF active chromophores of the molecule being studied. Using a similar experimental approach to that used in the SH experiments the absolute orientation of the terminal methyl group of pentadecanoic acid at the air/water interface was determined to be directed away from the air/water interface.⁵⁹ By using this result it was then shown that the terminal methyl group of a liquid crystal monolayer spread on quartz had the same phase and was therefore also directed away from the quartz substrate.

D. Chemical Reactions at Interfaces

Because of the unique geometrical structure, composition, and polarity of the interface, it is anticipated that chemical equilibria and the kinetics of chemical reactions will differ from the bulk phases that bound the interface. This has indeed been shown to be the case for a class of chemical reactions of considerable interest, namely acid–base reactions.

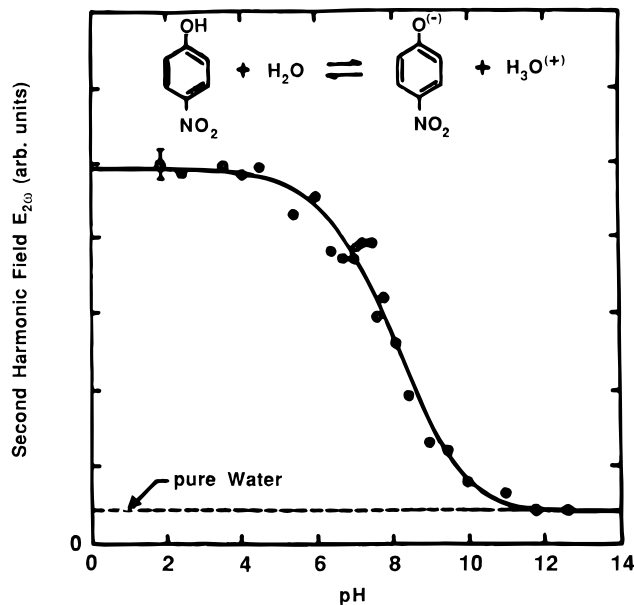


Figure 4. Amplitude of second-harmonic electric field at the air/aqueous solution interface of a nitrophenol in aqueous solution as a function of pH at 22 °C. The SH electric field is proportional to the populations of water and solutes adsorbed to the interface. (Reprinted from ref 60. Copyright 1987 American Institute of Physics.)

1. Acid–Base Equilibria: *p*-Nitrophenol at the Air/Water Interface

Although the first attempt to use SHG to measure interface acid–base equilibria was not successful, it was nonetheless of value in showing what was necessary to be able to study acid–base reactions and charged species in general at aqueous interfaces.⁶⁰ The negatively charged base *p*-nitrophenolate (*p*-NO₂-C₆H₄-O[−]) was not detected at the air/aqueous interface at high pH even though *p*-nitrophenolate was the dominant form (>99%) in the bulk solution. If *p*-NO₂-C₆H₄-O[−] was present at the interface then the SH signal would have been much greater than the signal observed, which was equal in magnitude to the signal from an air/neat water interface (Figure 4). Because of the greater solvation energy of the *p*-nitrophenolate ion in the bulk and its image repulsion at the interface, its population at the interface was too low to be detected above the SH background water signal. It is clear that in order to determine acid–base equilibria at an interface, or for that matter in a bulk phase, it is necessary to be able to measure the populations of the reactants and the products, both neutral and charged.

2. Charged Molecules at the Air/Water Interface and Interface *pK_a*

One approach to making charged molecules detectable at the air/water interface is to find some way to increase their interface population, especially if the SH sensitivity cannot be markedly improved. By attaching hydrophobic groups to a molecule, the surface population of the charged species can usually be increased sufficiently at the air/water interface to make it detectable. By using this approach an alkyl chain, which is hydrophobic, was attached in the para position of phenol and aniline to increase the interface populations of their respective charged forms^{61,62}

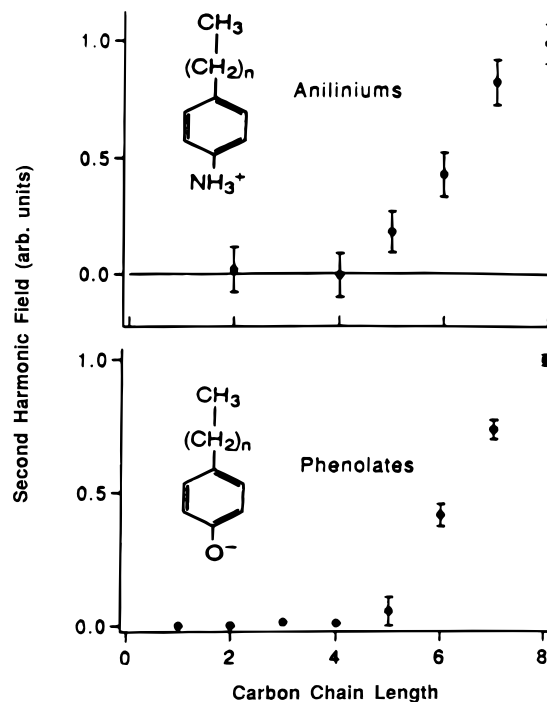


Figure 5. Amplitude of second-harmonic electric field, which is proportional to interface populations of adsorbate ions, as a function of carbon chain length for phenolate and anilinium ions in water. The contribution of water to the SH signal has been subtracted out. (Reprinted from ref 62. Copyright 1991 American Institute of Physics.)

(Figure 5). It was found that a minimum of five carbons were necessary to increase the interface population to a level sufficient to observe the charged forms, i.e. the pentyphenolate, CH₃(CH₂)₄-C₆H₄O[−], and the pentyanilinium, CH₃-(CH₂)₄-C₆H₄NH₃⁺.

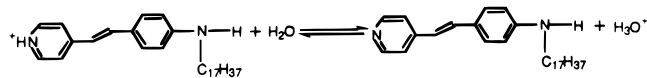
The connection between the interface populations of charged and neutral molecules and the driving force that determines their interface populations is given by the Gibbs adsorption free energy, $\Delta G^{\circ}_{\text{ADS}}$, which is the reversible work to bring a molecule from the bulk to the interface. For a charged molecule it has an electrostatic part $\Delta G^{\circ}_{\text{EL}}$, which is the reversible electrical work to bring a charge from the bulk, where the potential is zero, to the interface where the potential is $\Phi(0)$. The remaining contribution is referred to as the chemical part $\Delta G^{\circ}_{\text{CHEM}}$. The $\Delta G^{\circ}_{\text{EL}}$ is given by

$$\Delta G^{\circ}_{\text{EL}} = N_A z e \Phi(0) \quad (5)$$

where N_A is Avogadro's number and z is the valency of the ion. Measurements of the SH signal strength as a function of bulk alkylphenolate and alkyl-anilinium concentration, combined with the Langmuir adsorption model and the Guoy–Chapman model for the interface double layer were used to obtain the values of $\Delta G^{\circ}_{\text{CHEM}}$ and $\Delta G^{\circ}_{\text{EL}}$.⁶²

Applying this SH approach to hexadecylanilinium at the air/water interface yielded a *pK_a* value of 3.6, which is a factor of 50 more acidic than the bulk *pK_a* value of 5.3.⁶³ For octadecylphenol, CH₃(CH₂)₁₇-C₆H₄-OH, the acidity decreased by a factor of 50 from a bulk *pK_a* value of 10 to an interface *pK_a* of 11.7.⁶⁴ We thus see that the interface favors the neutral over the charged form in acid–base equilibria, as was found for *p*-nitrophenol⁶⁰ at the air/water interface.

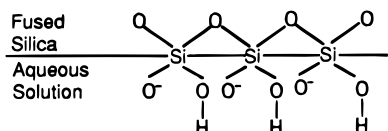
SH experiments have also shown that the interface acid–base equilibrium can be markedly shifted from its bulk value by controlling the interface environment.^{65,65a} It was observed that imbedding a hemicyanine molecule in a stearic acid monolayer, resulted in a large shift in the acid–base reaction



from a pK_a of 6.7 in bulk aqueous solution to 3.5 in the interface.

3. Acid–Base Equilibria at the Fused Silica/Water Interface: Polarization of Bulk Water Molecules

At the silica/water interface the silanol groups (SiOH), formed on exposure of silica to water, terminate the solid surface and are the acidic species in the interfacial acid–base chemistry.



From measurements of the SH amplitude as a function of bulk pH it was shown that the SH signal is generated not only by a second-order process that depends on the nonlinear polarizabilities $\alpha^{(2)}$ of the SiOH, SiO⁻, and water at the interface but also by a third-order process.^{66,67} This third-order process arises as the SiOH undergoes its acid–base reaction and produces the charged SiO⁻ group. The charged interface generates a large electric field E_0 , which extends into the bulk water, and polarizes and aligns the bulk water molecules, breaking the centrosymmetry of the bulk water phase. The field E_0 extends from several angstroms to hundreds of angstroms into the bulk solution depending on the electrolyte concentration and temperature. The total second harmonic field $E_{2\omega}$, which is proportional to the total nonlinear polarization $P_{2\omega}$ is given by

$$E_{2\omega} \propto P_{2\omega} = \chi^{(2)} E_{\omega} E_{\omega} + \chi^{(3)} E_{\omega} E_{\omega} \Phi(0) \quad (6)$$

where $\Phi(0)$ is the electrostatic potential at the interface and $\chi^{(3)}$ is the third-order susceptibility. It was found that including the polarization of the bulk water molecules gave quantitative agreement with the observed dependence of the SH signal on electrolyte concentration and temperature.⁶⁶ The results showed that two different silanol sites dominated the acid–base chemistry, one having a pK_a of 8.5, occupying 80% of the sites, and the other a pK_a of 4.5, occupying 20% of the sites⁶⁶ (Figure 6).

4. Sum Frequency Study of Acid–Base Equilibria

Just as SHG can be used to investigate acid–base equilibria, the pH-dependent changes in the SF spectrum can also be used. The acid–base properties of octadecylamine, CH₃(CH₂)₁₇NH₂, at the air/aqueous interface were investigated by monitoring the change in the vibrational spectrum as a function of bulk pH.⁶⁸ The amplitude of the symmetric methyl

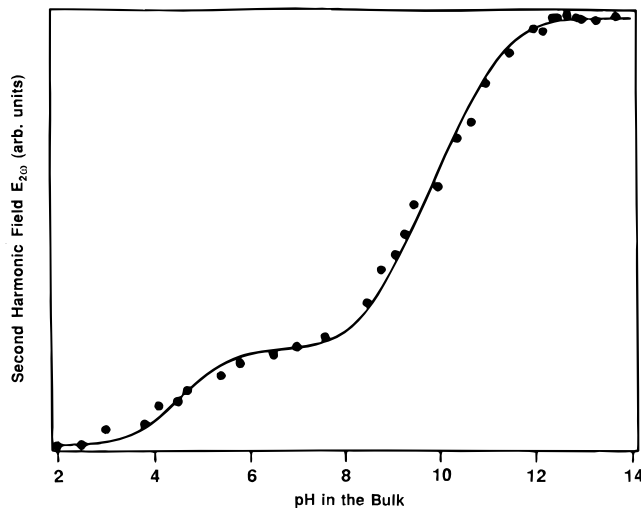


Figure 6. Acid–base equilibria experiment. Amplitude of second-harmonic electric field from amorphous silica (SiO₂)/H₂O interface as a function of bulk pH. The dots are experimental points and the solid line is a theoretical fit using a constant capacitance model for the electrical double layer, which results from the ionization of the interface silanol (–SiOH) groups. (Reprinted from ref 66. Copyright 1992 Elsevier.)

overtone normalized to the methyl symmetric stretch was used to monitor the surface density of the neutral amine. A sharp change in the methyl SF signal in the bulk pH range of 10 to 11 was attributed to the ionization of the amino group. This change, which occurs at a pH \approx 10.5 can be used to estimate the interface pK_a value, provided the interface pH_S is determined. One way to do this uses the Guoy–Chapman model to relate the interface pH_S to the bulk pH.⁶³

E. Electrochemistry

The application of SHG to electrochemical systems provides a new way to probe the electronic and structural properties of buried electrochemical surfaces in situ, a feature not available to most other methods. It provides new information on surface electronic properties beyond that of linear optical spectroscopic methods. Following early SH studies of semiconductor electrodes, there have been notable experimental and theoretical advances in studies of metal/electrolyte,^{4,69–73,73a} semiconductor/electrolyte interfaces,^{74–78} as well as the electrochemical interface between two immiscible electrolyte solutions.⁷⁹

1. Acid–Base Equilibria in an Electrochemical Cell

Just as a charged monolayer at an interface can alter acid–base equilibria,^{65,65a} the application of an external field across an interface can be used to effect acid–base changes. SH studies of the acid–base equilibria of a surfactant molecule 4-[4'-[(dodecyloxy)-azo]phenyl]benzoic acid at a 1,2-dichloroethane/water interface in an electrochemical cell explored the interplay of applied potential, interface pH and the interface populations of the acid–base pair⁷⁹ (Figure 7).

2. A Semiconductor/Liquid Interface: Si–SiO_x–SiO₂/Water

An interface of particular interest is the widely studied and used semiconductor, silicon, immersed

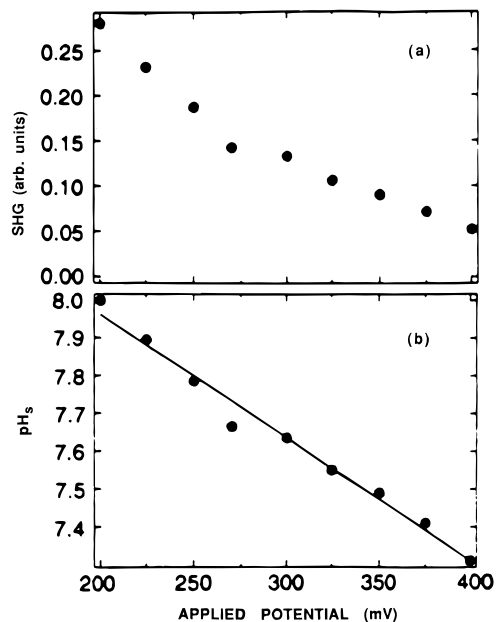


Figure 7. (a) SHG from a monolayer of the surfactant 4-(4'-[(dodecyloxy)azo]phenyl)benzoic acid at the water/dichloroethane interface as a function of applied potential. (b) Effective interface pH as a function of applied potential obtained from SH measurements of relative surface coverage. (Reprinted from ref 79. Copyright 1995 Chemical Society of London.)

in an aqueous electrolyte solution. The silicon typically becomes oxidized to SiO_2 , forming an outer layer of SiO_2 . It is the nonstoichiometric silicon oxide, SiO_x , transition layer, separating the silicon and SiO_2 , that is of critical importance in determining the electrochemical properties of the system. The thickness of the transition zone, perhaps 1–3 nm, as well as its exact composition and structure remain controversial. SHG and its dependence on applied potential is yielding information on the effects of the oxide, SiO_x , on the space charge in this interfacial region.⁷⁶

3. Surface Reconstruction

Studies of the adsorption of pyridine at single-crystal silver and gold/electrolyte interfaces by SHG has made it possible to probe the relation of molecular adsorption and surface reconstruction of these single-crystal electrodes.⁷⁰ For the Au(110) face the pyridine adsorption has a moderate effect on the reconstruction of the (110) face by formation of microfacets having (111) orientations.

F. Some Environmentally Interesting SH Studies

1. Corrosion

In studies of metal/liquid interfaces, SHG has been able to monitor the adsorption of a corrosion inhibitor onto steel.⁸⁰ SHG makes it possible to investigate the contribution of the different parts of an adsorbed molecule on the inhibition process; a potentially noteworthy advance in the study of this complex and environmentally important process.

2. Adsorption of Gas onto a Liquid Surface

The adsorption of gas-phase SO_2 molecules onto an air/water interface⁸¹ has been monitored in recent

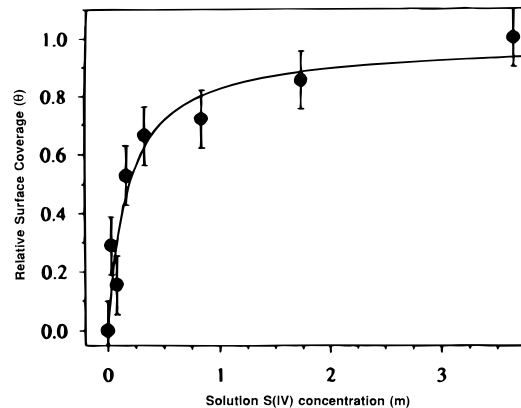


Figure 8. SHG determination of relative surface coverage (θ) as a function of the solution concentration (molality m) of sulfur in valence state IV. Dots are the experimental points and the solid line is a theoretical fit to the Langmuir adsorption isotherm. (Reprinted from ref 81. Copyright 1995 American Chemical Society.)

SHG experiments. This first demonstration of the applicability of SHG to a gas/liquid surface adsorption involving gas-phase molecules is of importance as a new way to directly probe the role of the surface in the transport of molecules between gas and liquid phases. The particular system, $\text{SO}_2(\text{gas})/\text{water}$ interface, is of particular importance because of the abundance of sulfuric acid aerosols and their role in atmospheric chemistry. The SH findings, which were obtained by using a resonance enhancement at the SO_2 absorption, indicate a surface layer of SO_2 whose adsorption to the air/water interface obeys a Langmuir adsorption isotherm (Figure 8).

G. Structural Phase Transitions

1. Langmuir Monolayers

The properties of insoluble monolayers, often called Langmuir monolayers, at air/water interfaces is a subject of longstanding interest as well as one of great current activity.⁹ The organization of the long-chain molecules comprising the monolayer can be described in terms of different phases, e.g. gas phase and various condensed phases referred to as "liquid" or "solid". The quasi-two-dimensional phase transitions connecting these various phases is of fundamental as well as practical importance. The phase diagrams of surface pressure vs monolayer density have served as a powerful way to study these two-dimensional structures. New approaches based on nonlinear spectroscopic methods have become available to study phase transitions in long-chain monolayers^{82–85a} and in liquid crystal films^{85b} at the air/water interface.

An early example was the use of SHG to observe the liquid expanded to liquid condensed, LE–LC, phase transition, which involves an increase in chain ordering in pentadecanoic acid, $\text{CH}_3(\text{CH}_2)_{13}\text{COOH}$, at the air/water interface.⁸² The new aspect that SHG was able to investigate was the change in molecular orientation of the carboxyl head group (orientation of the C–OH bond) from 45° to 60° with respect to the surface normal, as the transition from the liquid expanded to the liquid condensed phase occurred. The study supported the description of the phase

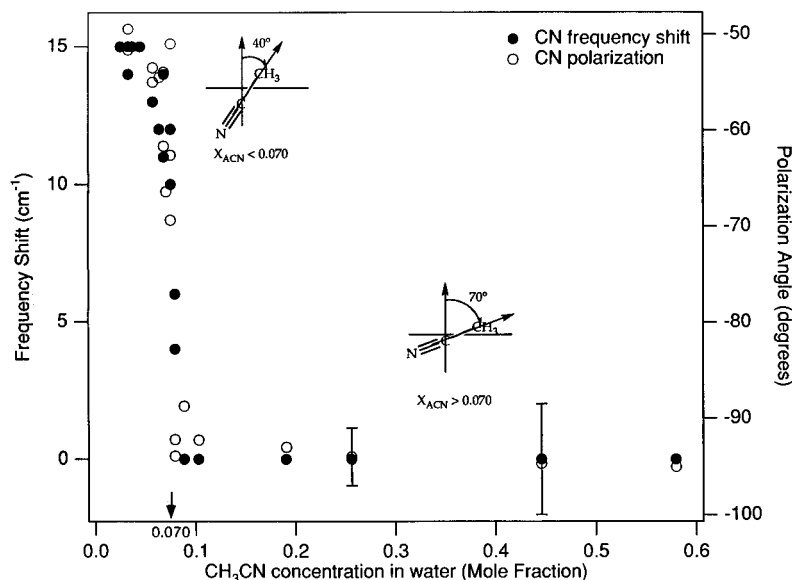


Figure 9. Structural phase transition at the air/acetonitrile–water interface observed by vibrational sum frequency generation. Solid circles are shifts in peak frequency of CN vibration for acetonitrile, CH_3CN , at air/acetonitrile–water interface relative to CN frequency in bulk acetonitrile. Unfilled circle shows polarization of SF light and is indicative of CH_3CN orientation at interface. At $X_{\text{CH}_3\text{CN}} < 0.07$, CH_3CN molecular angle is 40° to the normal and at $X_{\text{CH}_3\text{CN}} > 0.07$ the angle is 70° . (Reprinted from ref 86. Copyright 1993 American Institute of Physics.)

transition as first order with the LC phase being a higher density phase of greater orientational order.

2. Langmuir Monolayers—Orientational Phase Transitions

In the pentadecanoic acid monolayer phase transition described above, indeed for most Langmuir monolayer phase transitions, the order parameter is the density. This is manifested by the presence of an inhomogeneous coexistence region separating the two phases, e.g. gas–liquid, LE–LC, etc., as seen in a pressure–density phase diagram. For example in the inhomogeneous gas–liquid coexistence region the interface consists of clusters of the long chain surfactants at a “liquid” phase density interspersed among well-separated (gas-like) individual long-chain surfactant molecules. The transition from one of the pure phases to the mixed phase coexistence region is manifested by density fluctuations as the interface becomes inhomogeneous. These density fluctuations have been observed in a long-chain acid, $\text{CH}_3(\text{CH}_2)_{14}\text{COOH}$, at the air/water interface in SH experiments where the incident light was focused to micrometer dimensions.⁸³ The thermal motions of the clusters into and out of the irradiated region produced large fluctuations in the SH signal. The phase diagram, obtained from the fluctuations in the SH intensity as a function of surface density, was the same as that obtained from the surface pressure vs surface density phase diagram. Unlike the surface pressure–density measurements, which require physical contact with the interface, the SH fluctuation method has the advantage of being a remote, not a contact method, and does not involve any perturbation of the interface. It could therefore be of value in determining the phase diagram in special cases.

The SH fluctuation experiments yielded an unexpected result on compressing a hexadecylamine, $\text{CH}_3(\text{CH}_2)_{15}\text{C}_6\text{H}_4\text{NH}_2$, monolayer just past the end point of its gas–liquid coexistence region, i.e. into the

homogeneous liquid-phase region.^{84,85} New fluctuations appeared on further compressing the monolayer, which were not originating from density fluctuations but rather from orientational fluctuations, involving the aromatic head groups. A new orientational phase transition was discovered that was not revealed in the surface pressure–density phase diagram of hexadecylamine. Analysis of the decay time of the fluctuations by modification of the Landau–Ginzberg equation, was used to show that the transition was weakly first order.⁸⁵ A number of monolayers in addition to hexadecylamine were observed to undergo this orientational phase transition.⁸⁵ Other structurally similar monolayers did not.⁸⁵ The origin of the different behaviors has not been established.

3. Phase Transition of Small Soluble Molecules at Air/Liquid Interface

In SFG studies of the orientation and hydrogen bonding interactions of the methyl and cyano chromophores of acetonitrile, CH_3CN , at the air/acetonitrile–water solution interface, an abrupt change in the orientation, and chemical environment of acetonitrile was observed as the CH_3CN density was changed⁸⁶ (Figure 9). At bulk CH_3CN mole fractions below 0.07 it was found that the CH_3CN symmetry axis is oriented at 40° with respect to the surface normal and that the CN is hydrogen bonded and solvated by surrounding water molecules. At a 0.07 bulk mole fraction, which approximately corresponds to the formation of a full CH_3CN monolayer, the frequency of the CN vibration shows an abrupt red shift to a value, within experimental accuracy, equal to that of CN in neat bulk acetonitrile. The frequency of the CN group at the interface indicates that there is no hydrogen bonding to or solvation by the water molecules when the CH_3CN bulk mole fraction exceeds 0.07. In a similar way to the spectral shift there is an abrupt change in the molecular orienta-

tion from a tilt angle of 40° , observed at mole fractions below 0.07, to the much flatter orientation of 70° at higher concentrations. These sharp changes in orientation and spectra were attributed to a structural phase transition. The phase transition was described in terms of the hydrogen-bonding and solvation interactions of the CN head group with neighboring water molecules, competing with the dipole–dipole repulsive interactions among the CN head groups. At low surface densities the CN chromophores are surrounded by water molecules, hydrogen bonded, and tilted by 40° to the interface normal. As the nitrile surface density increases water molecules are squeezed out of the interface, the distances separating the aligned CN dipoles decrease, and the water screening of the nitriles is diminished. The result is to greatly increase the CN–CN dipole repulsions. At the phase transition density the large repulsive dipole–dipole interactions are relieved by the nitrile molecules reorienting toward the flatter and energetically more favorable head to tail dipole configuration. The trigger for the structural phase transition is this reorientation, which weakens or ruptures the hydrogen bonding to and solvation by neighboring water molecules resulting in the observed spectral red shifts in the CN vibrational frequency. This is the first case of a phase transition involving small mutually soluble molecules at a liquid interface.

H. Chiral Interfaces

The handedness or chirality of a molecule is a fundamental manifestation of its structure. In life processes the chirality of amino acids and various larger biological molecules, which make up living organisms, are well known. The interactions of various chiral molecules, whether natural or man made, such as drugs, with membrane and protein surfaces are of great importance in understanding many biological phenomena. Recent studies have shown that the use of circularly polarized light in a SH experiment can selectively probe the chirality of interfaces.^{87,88} This sensitivity to handedness is analogous to the linear spectroscopies of optical rotatory dispersion, ORD, and optical circular dichroism, CD, which are methods that have been used for many years to study the structure of bulk molecules. The rotation of linearly polarized light in ORD, and the difference in absorption by left- and right-handed circularly polarized light in CD, are dependent on the electric dipole and magnetic dipole transitions in the molecule of interest. In SHG-ORD⁸⁷ the rotation of the SHG light due to the chiral interface is measured, and in SHG-CD⁸⁸ the difference in the SH signal obtained using incident left-handed circularly polarized and right-handed circularly polarized light is measured. In the SHG-CD experiment the wavelength of the incident light is selected so that the second-harmonic light is resonant with an electronic transition of the interface molecules. Unlike the ORD and CD linear spectroscopies which are weak effects that show small angles of rotation and small differences in absorption by right vs left circularly polarized light, the SHG-ORD and SHG-CD yield large effects. For example in SHG-CD for a mono-

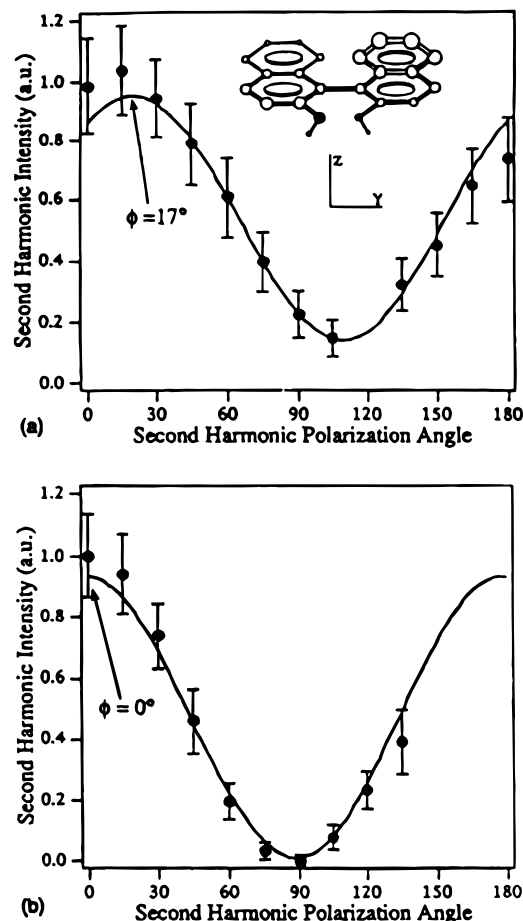
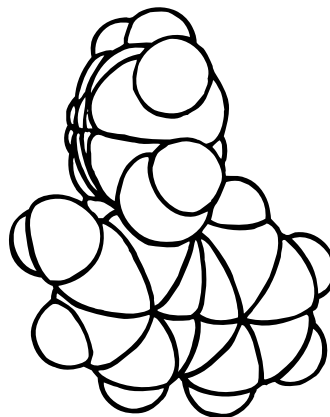


Figure 10. Second-harmonic optical activity at chiral and racemic interfaces. Optical rotation angle φ obtained from polarization of SH signals from air/water interface for saturated aqueous solutions: (a) (*R*)-2,2'-dihydroxy-1,1'-binaphthyl and (b) 50:50 racemic mixture of (*R*) and (*S*) forms. (Reprinted from ref 87. Copyright 1994 American Institute of Physics.)

layer of the *R* enantiomer of 2,2'-dihydroxy-1,1'-binaphthyl (BN) the left circularly polarized light



gave a SH signal five times that of right circularly polarized light.⁸⁸ In linear circular dichroism the difference in left vs right circularly polarized absorption divided by their absorption sum is typically in the range of 10^{-3} . Similarly linear ORD yields rotations of millidegrees, whereas SHG-ORD yields⁸⁷ rotations of the order of ten degrees (Figure 10). The large magnitude of the SHG-CD and SHG-ORD compared with linear CD and ORD, derives from the

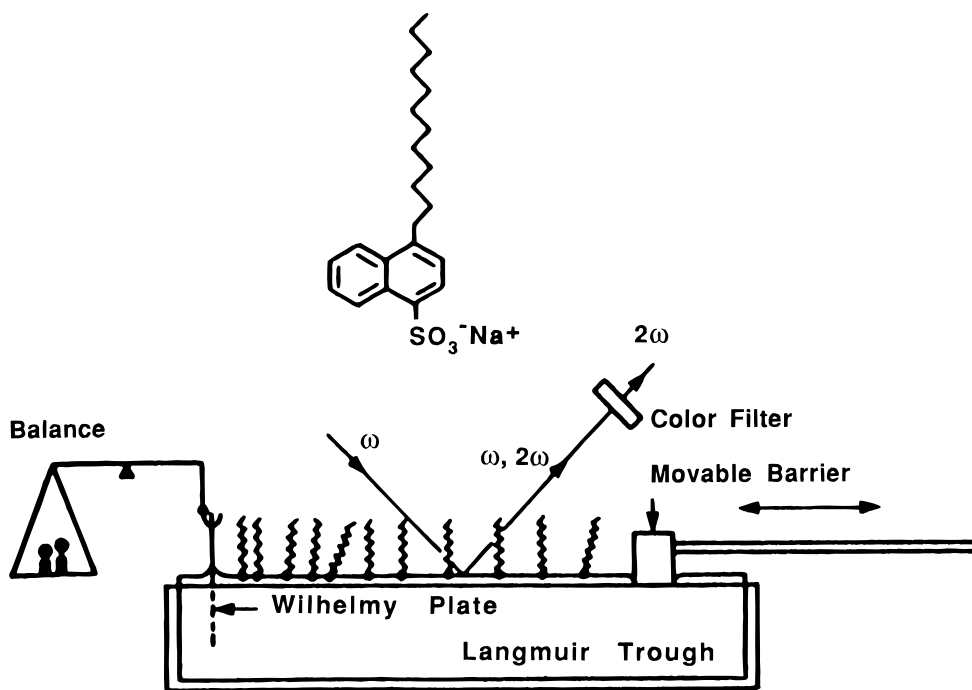


Figure 11. Schematic diagram for measuring adsorption kinetics of a monolayer of sodium 1-dodecyl-naphthalene-4-sulfonate from an aqueous solution to the air/water interface. (Reprinted from ref 89. Copyright 1988 American Institute of Physics.)

different origins of the linear and SH effects. For the nonlinear SH process the relevant $\chi^{(2)}$ elements contain only electric dipole transitions, unlike the linear spectroscopies where weak magnetic dipole transitions are involved in both the rotational strength and circular dichroism. Although the subject of SH chiral effects is in its infancy, its potential for studying the equilibrium and dynamic processes of chiral molecules at interfaces is most promising.

III. Dynamics at Liquid Interfaces

Second-harmonic and sum-frequency generation are particularly well-suited to investigate the kinetics of chemical and physical changes at interfaces. The pulses of light generated by picosecond and femtosecond lasers make it possible to achieve excellent time resolution. In addition the frequency tunability of lasers provides the spectral resolution necessary to identify the various chemical species at the interface that decay or form in the course of chemical reactions.

A. Adsorption Kinetics to Air/Water Interfaces

An interface that consists of molecules soluble in the bulk solution is constantly exchanging molecules with the bulk solution. At equilibrium the rates of adsorption to the interface from the bulk solution and desorption from the interface into the bulk solution must be equal for each chemical species. If the equilibrium interface population of one of the adsorbed molecular species is disturbed in some way then the kinetics of re-establishing equilibrium can be determined using SHG or SFG.

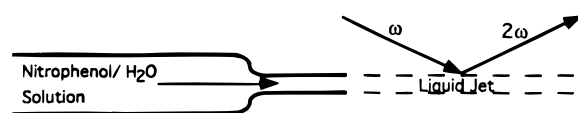
1. Surfactant Adsorption Kinetics

An air/water interface containing a monolayer of the long-chain surfactant sodium dodecyl-naphthalene-

lenesulfonate (SDS), $\text{CH}_3(\text{CH}_2)_{11}\text{-C}_{10}\text{H}_6\text{-SO}_3\text{Na}$, was made by preparing a saturated water solution of SDS in a Langmuir trough.⁸⁹ The interfacial equilibrium was disturbed by sweeping the surface with a movable barrier, which removed the SDS from the surface area to be investigated. Immediately following the SDS removal, the population kinetics at the interface was followed by measuring the time dependence of the SH signal (Figure 11). Because the bulk to interface adsorption is slow, the time it takes to sweep the surface did not limit the time resolution. A significant result was that the kinetics did not follow a $t^{1/2}$ dependence in the growth of the interface surfactant population. If the process was one-dimensional diffusion then a $t^{1/2}$ dependence would be expected. It was demonstrated that the kinetics could be fit to a Langmuir adsorption model with a fast and a slow rise time component.

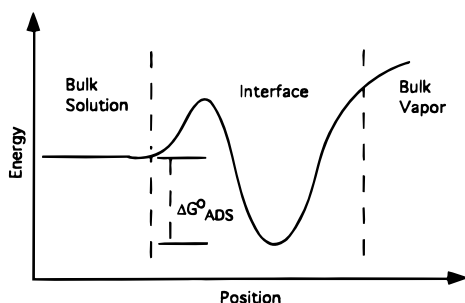
2. SHG and a Liquid Jet: Adsorption and Desorption

Unlike the long-chain molecules just discussed, the exchange kinetics of small molecules between the bulk and the interface is too fast to be observed by a perturbation method as slow as the sweeping of the surface with a mechanical barrier. One way that proved successful was to generate a liquid jet containing the surface active molecules of interest.⁹⁰ The air/liquid interface of a jet formed immediately after the nozzle yields an air/liquid interface that is initially not likely to have the molecules at their equilibrium interface populations or orientations.



The initial molecular orientations and populations at

the newly formed air/water interface are determined by the interactions and processes at the liquid–nozzle exit. The equilibrium population of molecules at the moving air/liquid jet interface takes time to develop. Measurement of the SHG signal at successive distances from the nozzle, in combination with the known flow rate of the jet, yields the time dependence of the SH signal.⁹⁰ By using an aqueous nitrophenol jet it was found that a time-dependent Langmuir model yielded an excellent fit to the data. Both an adsorption rate constant of $4.4 \pm 0.2 \times 10^4 \text{ s}^{-1}$ and a desorption rate constant of $6 \pm 2 \text{ s}^{-1}$ were obtained. The adsorption free energy was calculated from the kinetic data and found to be the same as the adsorption free energy obtained from equilibrium measurements of a static air/nitrophenol–water interface. This agreement in the static and dynamic free energy results supports the correctness of the kinetic model because the adsorption free energy must be the same whether measured by a dynamic method that gives the forward and backward rate constants, or the static equilibrium experiment that gives the ratio of the rate constants. It is the ratio that connects the equilibrium constant and the adsorption free energy. As with the surfactant SDS, the kinetics for the nitrophenol adsorption did not obey diffusion kinetics and indeed was much slower than predicted by a diffusion process. Although the motions of nitrophenol up to the vicinity of the interface are certainly diffusive, it has been proposed that an adsorption barrier of a few kilocalories/mole controlled the adsorption kinetics.⁹⁰



B. Electron Transfer at a Liquid/Liquid Interface

Electron transfer across an interface is a subject of considerable importance in the fundamental sciences and in technology. Depending on the composition and structure of the interface, the oxidation and reduction products of an electron-transfer reaction can be separated into the two adjacent bulk phases. One way to achieve this is to use an organic liquid/water interface with an electron donor that is soluble in only one of the liquid phases and an electron acceptor that is soluble only in the other liquid phase. One such system is the water/1,2-dichloroethane (DCE) interface with a ferrocene derivative that is only soluble in the organic phase and tris(2,2'-bipyridinyl)ruthenium(II) ($\text{Ru}(\text{bpy})_3^{2+}$), chloride that is only soluble in the water phase⁹¹ (Figure 12).

Because electron transfer is a short-range process the donor and acceptor molecules must be very close to the interface ($\sim 10 \text{ \AA}$) for the reaction to occur. For the ferrocene derivative– $\text{Ru}(\text{bpy})_3^{2+}$ pair the oxidation–reduction potentials do not permit electron transfer when they are in their ground electronic

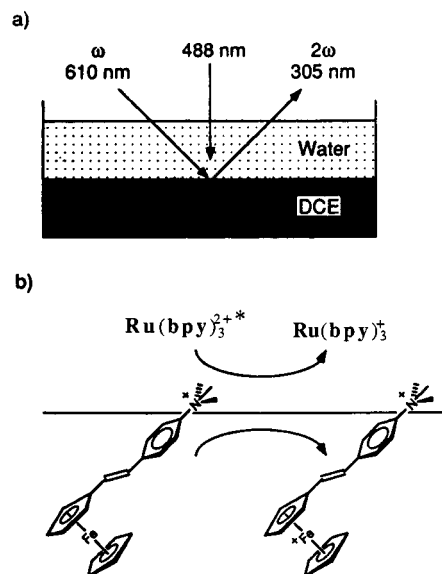


Figure 12. (a) SHG experiment for monitoring the photoinduced electron-transfer reaction from a 1+ ferrocene derivative to photoexcited $\text{Ru}(\text{bpy})_3^{2+}$ at a water/dichloroethane interface. (b) Schematic representation of the photoinduced electron transfer at a water/dichloroethane interface. (Reprinted from ref 91. Copyright 1993 American Chemical Society.)

states. To induce the electron-transfer process the electron acceptor $\text{Ru}(\text{bpy})_3^{2+}$ is photoexcited.⁹¹ The reaction is then energetically favorable when the ferrocene derivative donor and the excited $\text{Ru}(\text{bpy})_3^{2+}$ acceptor are in the vicinity of the interface (Figure 12).

The SH signal is shown to be due to the ferrocene derivative in its initial state of charge 1+ or in its oxidized state of 2+, with no contribution from the acceptor in its ground or excited states.⁹¹ Prior to excitation of $\text{Ru}(\text{bpy})_3^{2+}$ a probe beam gives a constant SH signal due to the donor in its initial 1+ state. On exciting the acceptor with a pump beam an increase in SH signal is observed as the donor (1+) transfers an electron to the excited acceptor at the interface. The increase arises from the increased nonlinearity of the donor in its oxidized state (2+). The rise time for the SH signal is $13 \pm 4 \text{ s}$ and is attributed to the time for the excited acceptor, $\text{Ru}(\text{bpy})_3^{2+*$, to diffuse to the interface where reaction can occur. The decay time of the SH signal, following the end of the photoexcitation, is $20 \pm 4 \text{ s}$. There are a number of processes that can contribute to this rate constant, including desorption of the oxidized donor from the interface, lateral diffusion of the oxidized donor from the irradiated area, and reduction of the donor back to its original state. Further studies on other donor–acceptor pairs at other liquid interfaces, with variations in interface composition, structure, and applied fields will further advance our understanding of the very important process of interfacial electron transfer.

C. Photoisomerization at Aqueous Interfaces

1. Barrier Crossing Dynamics—Polarity and Friction at the Interface

The kinetics of a liquid-state unimolecular chemical reaction, such as a photoisomerization, can often be

project into the air side of the interface. On the basis of this model it follows that for MG, the isomerization rate is determined in the higher friction water side of the interface, whereas for DODCI, the isomerization rate is determined in the lower friction air side of the interface.

At the silica/water interface the isomerization time for MG was found to increase to a value of 5.5 ps.⁹⁴ This slower isomerization could reflect the increased water structure, suggested in fluorescence studies near the silica/water interface,^{95,96} or it could be due to specific interactions of MG with the silica. At the silica/ether interface a SH study^{96a} revealed an isomerization time (40 ps), which is much longer than expected in bulk ether. The effects of interface aggregates at the high MG concentrations used, specific interactions of MG with silica, or the structure of ether at the interface remain to be established.

D. Orientational Relaxation at the Air/Water Interface

Ever since the development of picosecond lasers, the rotational motion of molecules has been and continues to be an important way to investigate intermolecular forces in bulk liquids and in the restricted environments of membranes, micelles, and vesicles. Unfortunately the powerful methods of fluorescence depolarization and transient dichroism or birefringence cannot generally be used at interfaces if the molecules of interest are also present in the bulk liquid. To avoid the overwhelming signal from the bulk molecules the method of restricting a fluorescent molecule to the interface by covalently attaching it to an insoluble long-chain surfactant has been used.⁹⁷ However the effect of bonding the fluorescent probe molecule to an insoluble surfactant is to restrict the probe molecule from undergoing the free rotational motion due to its intermolecular interactions with solvent molecules and other molecules at the interface.

Another method, which seeks to minimize the excitation of bulk molecules, involves an evanescent wave technique, i.e. total internal reflection. However the evanescent wave method is generally not interface specific because the evanescent wave penetrates to a distance of the order of $\lambda/2$ into the bulk solution, which is typically of the order of 1000 Å. Thus many bulk molecules are usually excited, which makes it difficult to determine the interface contribution. However when the adsorption of a probe molecule to the interface is so strongly favored that there is only a very small bulk concentration (10^{-8} – 10^{-9} M) the fluorescence originating from the bulk molecules can be neglected. Some very interesting results have been obtained on reorientation of acridine orange at silica/water^{97a} and liquid alkane/water^{97b} interfaces using this approach.

By using a pump–SHG probe method it has been demonstrated that the rotation of molecules in the interface can be observed, even when there is a large population in the bulk solution.⁹⁸ In the pump–SHG probe method an ultrashort light pulse is used to disturb, by photoselective excitation, the equilibrium orientation of interfacial molecules (Figure 15). The

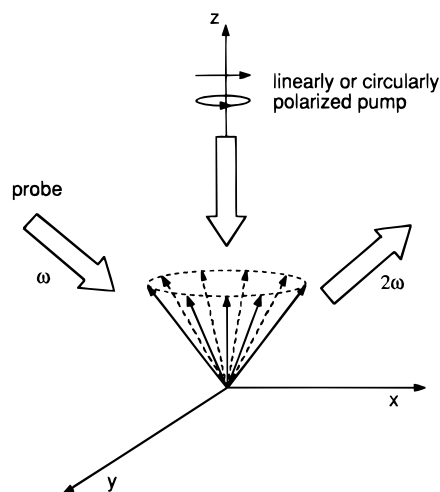


Figure 15. Schematic of SH experiment for measuring interfacial molecular reorientation dynamics. The arrows show one tilt angle of the orientational distribution of the molecular transition dipoles before photoexcitation. (Reprinted from ref 98. Copyright 1991 American Chemical Society.)

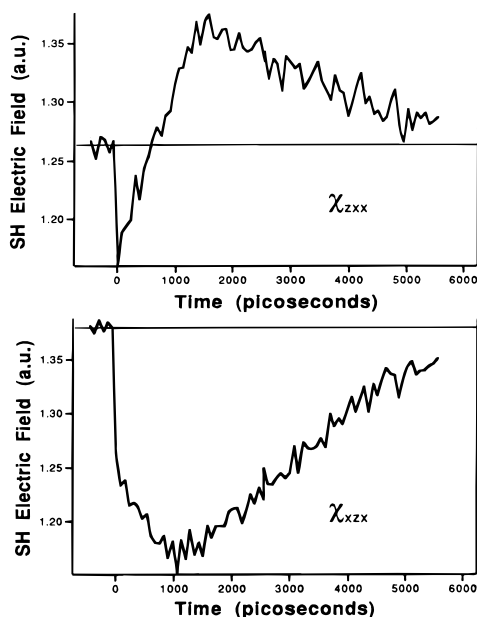


Figure 16. Time dependence of different polarization elements, $\chi^{(2)}_{zxx}$ and $\chi^{(2)}_{xzx}$, obtained in photoexcitation pump–SH probe experiment for rhodamine-6G at the air/water interface. Z is the laboratory axis normal to the interface and X is an axis in the plane of the interface. (Reprinted from ref 98. Copyright 1991 American Chemical Society.)

orientational relaxation of rhodamine-6G (Rh-6G) at the air/water interface was obtained from measurements of the second-harmonic light generated by a probe pulse that was time delayed with respect to the photoexciting pump pulse (Figure 16). The orientational relaxation time of Rh-6G at the air/water interface was found to be in the range of several hundred picoseconds (400–500 ps), which is longer than in bulk water (200 ps).^{98a} However it is necessary to recognize in any comparison of rotational times from fluorescence and SH methods that the SH method probes a different moment of the orientational motion than the fluorescence method. Different rotational time constants could therefore

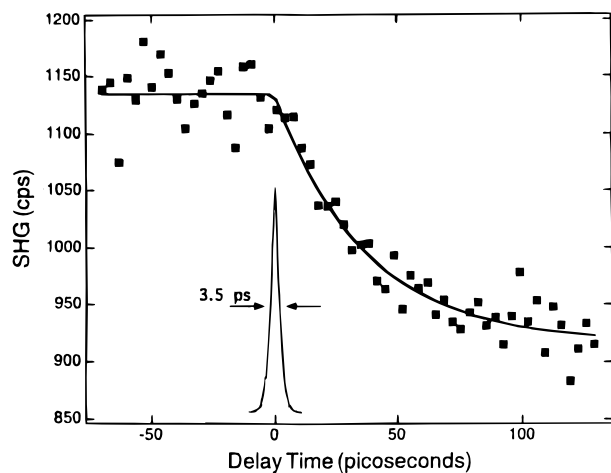


Figure 17. Time-dependent measurement of the transport of photogenerated holes to the n -TiO₂ electrode/electrolyte interface in a photoexcitation of n -TiO₂-SH probe experiment. The solid line gives an exponential fit of 36 ps. The sharp peak shows the instrument response. (Reprinted from ref 78. Copyright 1995 American Chemical Society.)

be obtained. In addition a model of the interface motion that includes the asymmetric force field at the interface, which favors certain molecular orientations, together with the intermolecular time-varying torques due to interactions with interfacial molecules is needed to extract the rotational time constants. One model for the interfacial rotational motions that could be applicable is rotational diffusion in the external force field due to the asymmetric interface.

Aside from the "slower" rotational motion at the interface, the results of the SH study suggest that the equilibrium orientation of the photoexcited Rh-6G molecules is different from that of the ground-state Rh-6G molecules. The change in molecular charge distribution on photoexcitation affects the intermolecular interactions with surrounding interfacial molecules and, because of the sensitivity of orientation to charge distribution, could readily shift the equilibrium orientation of the excited molecule from the ground state value. In addition the rotational motions appear to be dominated by motions out of the interface plane based on the kinetics being the same for a linearly polarized pump beam and a circularly polarized pump beam. It seems clear from this early study that the application of the pump-SH or SF probe method to the study of rotational motions at various liquid interfaces promises to be important in investigating interfacial forces, friction at interfaces, and the relation of hydrodynamic transport quantities such as interfacial viscosity to interfacial friction.

E. Photogeneration of Charges at a Semiconductor/Water Electrochemical Interface

A picosecond pump-SH probe experiment of the n -TiO₂ semiconductor electrode/electrolyte interface provides new information on the interface electric fields and the motion of holes in the semiconductor.⁷⁸ Following the pump UV photogeneration of a large hole population, the time-delayed SH probe measured the transit time of the photogenerated holes to the electrode/electrolyte interface (Figure 17). An aver-

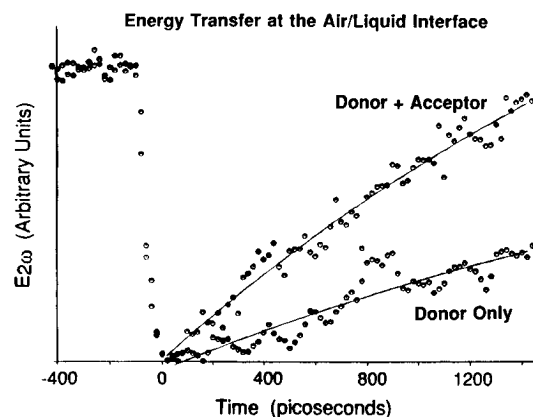


Figure 18. Amplitude of second-harmonic electric field vs time in an energy-transfer experiment at the air/water interface. Pump pulse excites rhodamine-6G at $t = 0$. The decay in presence and absence of DODCI acceptor is shown. The solid line in the absence of acceptor fits an exponential with $\tau = 3.1$ ns. The solid line for donor + acceptor is fitted to eq 7 of text. (Reprinted from ref 99. Copyright 1989 American Institute of Physics.)

age transit time of 25 ps was observed from a calculated escape depth of 20 nm from the TiO₂ electrode surface. These measurements, which are the first time-dependent SH studies of the semiconductor electrode/electrolyte interface, demonstrate the capability of SHG to probe semiconductor electrodes.

F. Dynamics of Intermolecular Energy Transfer

In bulk media the intermolecular transfer of energy is an important step in excited-state deactivation and in photochemical reactions. The energy transfer can occur by a long-range dipole-dipole (Förster) mechanism, or a short-range exchange mechanism. To study intermolecular energy transfer at the air/water interface the donor Rh-6G and the acceptor DODCI were used. The donor Rh-6G was selectively pumped with a picosecond laser pulse and a time-delayed picosecond pulse served as a SH probe of the time-dependent Rh-6G population.⁹⁹ The SH signal due to the acceptor DODCI was shown to be negligible compared with the signal due to Rh-6G. The bulk concentrations were kept sufficiently low that energy transfer between interface and bulk molecules was effectively eliminated. The relatively strong adsorption of the donor-acceptor pair to the interface resulted in much smaller average donor-acceptor distances than in the bulk solution. In the bulk solution the donor decay rate increased by only 15% when the acceptor was present, whereas at the interface there was a large change, roughly a factor of 3, in the donor decay rate (Figure 18). The contribution of donor-donor transfers to the overall donor-acceptor transfer was not important as seen in varying the donor concentration. An analysis of the transfer dynamics in terms of a two-dimensional (2D) Förster transfer vs a three-dimensional (3D) Förster transfer indicated that the parameters used in the fitting for the 2D model were more reasonable than for the 3D model (Figure 18). For the 2D-Förster model the decay of the donor is given by

$$D(t) = D(0) \exp[-t/\tau_0 - b(t/\tau_0)^{1/3}] \quad (7)$$

where τ_0 is the donor lifetime in the absence of

acceptors, and the coefficient b contains the donor–acceptor coupling strength, the donor–acceptor orientational factor, and the acceptor interface density. Although the fit to the 2D model seems good, the assumptions implicit in the use of a 2D-Förster transfer model requires not only further investigation, but development of a more complete treatment of what appears to be a quasi 2D energy-transfer process.

IV. Summary

Although only a restricted range of chemical and physical topics have been described in this article, we see that the relatively new spectroscopies of second-harmonic and sum-frequency generation have markedly changed and expanded the fields of interfacial chemistry, physics, and biology. The possibilities for studying equilibrium and dynamic processes at the molecular level continues to grow rapidly. The high power, tunability, and time resolution of commercially available lasers makes it possible to selectively excite and to study interfacial molecules using the nonlinear optical methods of SHG and SFG. The capability of these methods to probe buried interfaces as well as exposed interfaces in a nonintrusive way establishes their particular value. Further progress in the application of the SH and SF methods will be provided by the development of new materials, and structures, including polymers and semiconductors, whose interfacial properties are of special interest. As the experimental side of this field grows the need for further theoretical and computer modeling of interfaces grows as well. If the next decade of research, both experimental and theoretical, increases as this last decade, we can anticipate significant advances in our understanding of interface phenomena, the discovery of new effects at interfaces, and the development of ideas for new technologies.

V. Acknowledgments

The author thanks the Division of Chemical Science of the Department of Energy and the National Science Foundation for their support. The author thanks Dr. E. Borguet for his assistance.

VI. References

- Bloembergen, N.; Pershan, P. S. *Phys. Rev.* **1962**, *128*, 606.
- Bloembergen, N. *Nonlinear Optics*; Wiley: New York, 1965.
- Williams, D. J., Ed. *Nonlinear Optical Properties of Organic and Polymeric Materials*; ACS Symposium Series 233; Washington, DC: American Chemical Society 1985.
- Richmond, G. L.; Robinson, J. M.; Shannon, V. L. *Prog. Surf. Sci.* **1988**, *28*, 1.
- Shen, Y. R. *Annu. Rev. Phys. Chem.* **1989**, *40*, 327.
- Heinz, T. F. In *Nonlinear Surface Electromagnetic Phenomena*; Ponath, H. E., Stegeman, G. I., Eds.; North Holland: Amsterdam, 1991; p 353.
- Eisenthal, K. B. *Annu. Rev. Phys. Chem.* **1992**, *43*, 627.
- Corn, R. M.; Higgins, D. A. *Chem. Rev.* **1994**, *94*, 107.
- Adamson, A. W. *Physical Chemistry of Surfaces*, 4th ed.; Wiley: New York, 1982. (a) Nguyen, D. C.; Muenchausen, R. E.; Keller, R. A.; Nogar, N. S. *Opt. Commun.* **1986**, *60*, 111.
- Heinz, T. F.; Tom, H. W. K.; Shen, Y. R. *Phys. Rev. A* **1983**, *28*, 1883.
- Hicks, J. M.; Kemnitz, K.; Heinz, T. F.; Eisenthal, K. B. *J. Phys. Chem.* **1986**, *90*, 560.
- Lee, C. Y.; Scott, H. L. *J. Chem. Phys.* **1980**, *83*, 4591.
- Stillinger, F. H.; Ben-Naim, A. *J. Chem. Phys.* **1967**, *47*, 4431.
- Fletcher, N. H. *Philos. Mag.* **1968**, *18*, 1287.
- Croxtan, C. A. *Physica A* **1981**, *106A*, 239.
- Townsend, R. M.; Gryko, J.; Rice, S. A. *J. Chem. Phys.* **1985**, *82*, 4391.
- Wilson, M. A.; Pohorille, A.; Pratt, L. R. *J. Phys. Chem.* **1987**, *91*, 4873.
- Brodskaya, E. N.; Rusanov, A. I. *Mol. Phys.* **1987**, *62*, 251.
- Linse, P. *J. Chem. Phys.* **1987**, *86*, 4177.
- Matsumoto, M.; Kataoka, J. *J. Chem. Phys.* **1988**, *88*, 3233.
- Meyer, M.; Mareschal, M.; Hayoun, M. *J. Chem. Phys.* **1988**, *89*, 1067.
- Gao, J.; Jorgensen, W. L. *J. Phys. Chem.* **1988**, *92*, 5813.
- Carpenter, I. L.; Hehre, W. J. *J. Phys. Chem.* **1990**, *94*, 531.
- Smit, B.; Hillers, A. J.; Esselink, K.; Rupert, L. A. M.; van Os, N. M.; Schlijper, A. G. *J. Phys. Chem.* **1991**, *95*, 6361.
- Benjamin, I. *J. Chem. Phys.* **1991**, *94*, 662.
- Pohorille, A.; Benjamin, I. *J. Chem. Phys.* **1991**, *94*, 5599.
- Yang, B.; Sullivan, D. E.; Tjijto-Margo, B.; Gray, C. G. *J. Phys.: Condens. Matter* **1991**, *3*, F109.
- Rose, D. A.; Benjamin, I. *J. Phys. Chem.* **1992**, *96*, 9561.
- Benjamin, I. *J. Chem. Phys.* **1992**, *97*, 1432.
- Pohorille, A.; Wilson, M. A. *J. Mol. Struct.* **1993**, *284*, 271.
- van Buuren, A. R.; Marrink, S. J.; Berendsen, J. C. *J. Phys. Chem.* **1993**, *97*, 9206.
- Pohorille, A.; Benjamin, I. *J. Phys. Chem.* **1993**, *97*, 2664. (a) Zhang, Y.; Feller, S. E.; Brooks, B. R.; Pastor, R. W. *J. Chem. Phys.* **1995**, *103*, 10252. (b) Feller, S. E.; Zhang, Y.; Pastor, R. W. *J. Chem. Phys.* **1995**, *103*, 10267.
- Higgins, D. A.; Abrams, M. B.; Byerly, S. K.; Corn, R. M. *Langmuir* **1992**, *8*, 1994. (a) Bell, A. J.; Frey, J. G.; Vandernoot, T. *J. Chem. Soc. Faraday Trans.* **1992**, *88*, 2027.
- Grubb, S. G.; Kim, M. W.; Raising, Th.; Shen, Y. R. *Langmuir* **1988**, *4*, 452.
- Higgins, D. A.; Corn, R. M. *J. Phys. Chem.* **1993**, *97*, 489.
- Guyot-Sionnest, P.; Shen, Y. R. *Phys. Rev. B* **1987**, *35*, 4420. (a) Luca, A. A. T.; Hébert, P.; Brevet, P. F.; Girault, H. H. *J. Chem. Soc., Faraday Trans.* **1995**, *91*, 1763.
- Conboy, J. C.; Daschbach, J. L.; Richmond, G. L. *J. Phys. Chem.* **1994**, *98*, 9688. (a) Hsuing, H.; Beckerbauer, R. *Chem. Phys. Lett.* **1992**, *193*, 123.
- Frynsinger, G. S.; Barnoski, A. A.; Gaines, G. L., Jr.; Korenowski, G. M. *Langmuir* **1994**, *10*, 2277. (a) Kim, M. W.; Liu, S. N.; Chung, T. C. *Phys. Rev. Lett.* **1988**, *60*, 2745.
- Eijt, S. W. H.; Witterbrood, M. M.; DeVillers, M. A. C.; Raising, Th. *Langmuir* **1994**, *10*, 4498.
- Kemnitz, K.; Bhattacharyya, K.; Hicks, J. M.; Pinto, G. R.; Eisenthal, K. B.; Heinz, T. F. *Chem. Phys. Lett.* **1986**, *131*, 285.
- Hicks, J. M.; Kemnitz, K.; Bhattacharyya, K.; Eisenthal, K. B. Unpublished results.
- Huang, J. Y.; Lewis, A. *Biophys. J.* **1989**, *55*, 835.
- Randles, J. E. B. *Phys. Chem. Liq.* **1977**, *7*, 107.
- Eley, D. D.; Evans, M. J. *Trans. Faraday Soc.* **1983**, *34*, 1093.
- Saloman, M. J. *J. Phys. Chem.* **1970**, *74*, 2519.
- Gomer, R.; Tryson, G. *J. Chem. Phys.* **1977**, *66*, 4413.
- Borazio, A.; Farrell, J. R.; McTigue, P. J. *Electroanal. Chem.* **1985**, *193*, 103.
- Zhou, Y.; Stell, G.; Friedman, H. L. *J. Chem. Phys.* **1988**, *89*, 3836.
- Goh, M. C.; Hicks, J. M.; Kemnitz, K.; Pinto, G. R.; Heinz, T. F.; Bhattacharyya, K.; Eisenthal, K. B. *J. Phys. Chem.* **1988**, *92*, 5074.
- Zhu, X. D.; Suhr, H.; Shen, Y. R. *Phys. Rev. B* **1987**, *35*, 3047.
- Hunt, J. H.; Guyot-Sionnest, P.; Shen, Y. R. *Chem. Phys. Lett.* **1987**, *133*, 189.
- Stanners, C. D.; Du, Q.; Chin, R. P.; Cremer, P.; Somorjai, G. A.; Shen, Y. R. *Chem. Phys. Lett.* **1995**, *232*, 407.
- Wolfrum, K.; Graener, H.; Laubereau, A. *Chem. Phys. Lett.* **1993**, *213*, 41.
- Du, Q.; Superfine, R.; Freysz, E.; Shen, Y. R. *Phys. Rev. Lett.* **1993**, *70*, 2313.
- Ong, T. H.; Davies, P. B.; Bain, C. D. *Langmuir* **1993**, *9*, 1836.
- Ward, R. N.; Davies, P. B.; Bain, C. D. *J. Phys. Chem.* **1993**, *97*, 7141.
- Bain, C. D.; Davies, P. B.; Ward, R. N. *Langmuir* **1994**, *10*, 2060.
- Ward, R. N.; Duffy, D. C.; Davies, P. B.; Bain, C. D. *J. Phys. Chem.* **1994**, *98*, 8536. (a) Du, Q.; Freysz, E.; Shen, Y. R. *Science* **1994**, *264*, 826.
- Superfine, R.; Huang, J. Y.; Shen, Y. R. *Opt. Lett.* **1990**, *15*, 1276.
- Bhattacharyya, K.; Sitzmann, E. V.; Eisenthal, K. B. *J. Chem. Phys.* **1987**, *87*, 1442.
- Bhattacharyya, K.; Castro, A.; Sitzmann, E. V.; Eisenthal, K. B. *J. Chem. Phys.* **1988**, *89*, 3376.
- Castro, A.; Bhattacharyya, K.; Eisenthal, K. B. *J. Chem. Phys.* **1991**, *95*, 1310.
- Zhao, X.; Subrahmanyam, S.; Eisenthal, K. B. *Chem. Phys. Lett.* **1990**, *171*, 558.
- Subrahmanyam, S.; Zhao, X.; Eisenthal, K. B. Unpublished results.
- Xiao, X. D.; Vogel, V.; Shen, Y. R.; Marowski, G. *Chem. Phys. Lett.* **1989**, *163*, 555. (a) Xiao, X. D.; Vogel, V.; Shen, Y. R.; Marowski, G. *J. Chem. Phys.* **1991**, *94*, 2315.

- (66) Ong, S.; Zhao, X.; Eisenthal, K. B. *Chem. Phys. Lett.* **1992**, *191*, 327.
- (67) Zhao, X.; Ong, S.; Eisenthal, K. B. *Chem. Phys. Lett.* **1993**, *202*, 513.
- (68) Wolfrum, K.; Löbau, J.; Laubereau, A. *Appl. Phys. A* **1994**, *59*, 605.
- (69) Schmickler, W.; Urbakh, M. *Phys. Rev. B* **1993**, *47*, 6644.
- (70) Lipkowski, J.; Stolberg, L.; Yang, D. F.; Pettinger, B.; Mirwald, S.; Henglein, F.; Kolb, D. M. *Electrochim. Acta* **1994**, *39*, 1045.
- (71) Nagy, G.; Roy, D. *Langmuir* **1993**, *9*, 1868.
- (72) Guyot-Sionnest, P.; Tadjeddine, A. *Chem. Phys. Lett.* **1990**, *172*, 341.
- (73) Bradley, R. A.; Georgiadis, R.; Kevan, S. D.; Richmond, G. L. *J. Chem. Phys.* **1993**, *99*, 5535. (a) Chen, C. K.; Heinz, T. F.; Ricard, D.; Shen, Y. R. *Phys. Rev. Lett.* **1981**, *46*, 1010.
- (74) Lee, C. H.; Chang, R. K.; Bloembergen, N. *Phys. Rev. Lett.* **1967**, *18*, 167.
- (75) Krüger, J.; Sorg, N.; Kautek, W. *Appl. Surf. Sci.* **1993**, *69*, 388.
- (76) Fischer, P. R.; Daschbach, J. L.; Gragson, D. E.; Richmond, G. L. *J. Vac. Sci. Technol. A* **1994**, *12*, 2617.
- (77) Kautek, W.; Sorg, N.; Krüger, J. *Electrochim. Acta* **1994**, *39*, 1245.
- (78) Lantz, J. M.; Corn, R. M. *J. Phys. Chem.* **1994**, *98*, 9387.
- (79) Naujok, R. R.; Higgins, D. A.; Hanken, D. G.; Corn, R. M. *J. Chem. Soc. Faraday Trans.* **1995**, *91*, 1411.
- (80) Klenerman, D.; Hodge, J.; Joseph, M. *Corros. Sci.* **1994**, *36*, 301.
- (81) Donaldson, D. J.; Guest, J. A.; Goh, M. C. *J. Phys. Chem.* **1995**, *99*, 9313.
- (82) Raising, Th.; Shen, Y. R.; Kim, M. W.; Grubb, S. *Phys. Rev. Lett.* **1985**, *55*, 2903.
- (83) Zhao, X.; Goh, M. C.; Subrahmanyam, S.; Eisenthal, K. B. *J. Phys. Chem.* **1990**, *94*, 3370.
- (84) Zhao, X.; Subrahmanyam, S.; Eisenthal, K. B. *Phys. Rev. Lett.* **1991**, *67*, 2025.
- (85) Zhao, X.; Eisenthal, K. B. *J. Chem. Phys.* **1995**, *102*, 5818. (a) Zhang, D.; Gutow, J.; Eisenthal, K. B. *J. Phys. Chem.* **1994**, *98*, 13729. (b) Xue, J.; Jung, C. S.; Kim, M. W. *Phys. Rev. Lett.* **1992**, *69*, 474.
- (86) Zhang, D.; Gutow, J. H.; Eisenthal, K. B.; Heinz, T. F. *J. Chem. Phys.* **1993**, *98*, 5099.
- (87) Byers, J. D.; Yee, H. I.; Hicks, J. M. *J. Chem. Phys.* **1994**, *101*, 1.
- (88) Petralli-Mallow, T.; Wong, T. M.; Byers, J. D.; Yee, H. I.; Hicks, J. M. *J. Phys. Chem.* **1993**, *97*, 1383.
- (89) Raising, Th.; Stehlin, T.; Shen, Y. R.; Kim, M. W.; Valint, P., Jr. *J. Chem. Phys.* **1988**, *89*, 3386.
- (90) Castro, A.; Ong, S.; Eisenthal, K. B. *Chem. Phys. Lett.* **1989**, *163*, 412.
- (91) Kott, K. L.; Higgins, D. A.; McMahon, R. J.; Corn, R. M. *J. Am. Chem. Soc.* **1993**, *115*, 5342.
- (92) Sitzmann, E. V.; Eisenthal, K. B. *J. Phys. Chem.* **1988**, *92*, 4579.
- (93) Sitzmann, E. V.; Eisenthal, K. B. Unpublished results.
- (94) Shi, X.; Borguet, E.; Tarnowski, A. N.; Eisenthal, K. B. *Chem. Phys.* **1996**, *205*, 167. (a) Saikan, S.; Sei, J. *J. Chem. Phys.* **1983**, *79*, 4154. (b) Migus, A.; Antonetti, A.; Etchepare, J.; Hulin, D.; Orszag, A. *J. Opt. Soc. Am. B* **1985**, *2*, 584. (c) Mokhtari, A.; Fini, L.; Chesnoy, J. *J. Chem. Phys.* **1987**, *87*, 3429.
- (95) Filligim, T. S.; Zhu, S. B.; Yao, S.; Lee, J.; Robinson, G. W. *Chem. Phys. Lett.* **1989**, *161*, 444.
- (96) Yanagimachi, M.; Tamai, N.; Masuhara, H. *Chem. Phys. Lett.* **1992**, *200*, 469. (a) Meech, S. R.; Yoshihara, K. *Chem. Phys. Lett.* **1990**, *174*, 423.
- (97) Anfinrud, P. A.; Hart, D. E.; Struve, W. S. *J. Phys. Chem.* **1988**, *92*, 4067. (a) Wirth, M. J.; Burbage, J. D. *J. Phys. Chem.* **1992**, *96*, 9022. (b) Wirth, M. J.; Burbage, J. D. *Anal. Chem.* **1991**, *63*, 1311.
- (98) Castro, A.; Sitzmann, E. V.; Zhang, D.; Eisenthal, K. B. *J. Phys. Chem.* **1991**, *95*, 6752. (a) Berndt, K.; Durr, H.; Palme, D. *Opt. Commun.* **1982**, *42*, 419.
- (99) Sitzmann, E. V.; Eisenthal, K. B. *J. Chem. Phys.* **1989**, *90*, 2831.

CR9502211